

Optimal Control of the Thrusted Skate^{*}

Kevin M. Lynch^a

^a*Mechanical Engineering Department, Northwestern University, Evanston, IL 60208 USA*

Abstract

This paper derives optimal controls for the *thrusted skate* between any two points in the plane. The thrusted skate consists of a skate, which steers the motion in \mathbb{R}^2 , and a fixed-orientation thruster which provides the power to move the system. This system is a simple example of a class of fully-actuated mechanical systems consisting of a single power actuator and a number of workless steering actuators which guide the motion of the system.

Key words: Optimal trajectory planning, workless steering actuators

1 Introduction

We are interested in motion planning for a class of fully-actuated mechanical systems where one actuator (the *power actuator*) provides power to drive the system and the rest of the actuators (the *steering actuators*) set up workless kinematic constraints constraining the motion of the system to a programmable one-dimensional curve in the configuration space. An example of such a system is the 3R robot arm developed by Moore *et al.* [5]. Continuously variable transmissions are used to set the ratios of angular velocities of the joints, constraining the velocity of the robot to be tangent to a curve in the configuration space. A single power motor is used to drive the robot along the curve. Because the steering actuators do no work, the energy expended in the motion is dominated by the energy to drive the power motor.

In this paper we study the two degree-of-freedom *thrusted skate* (Figure 1), a simple example of such a system. The configuration of the system is given by the location of its center of mass $(x, y) \in \mathbb{R}^2$. The power actuator is the thruster, and the one steering actuator is the skate (or wheel). The thruster provides a force u through the center of mass and aligned with the y -axis. The angle of the skate θ controls the direction of free motion of the system. The system moves freely and without friction in the direction the skate is pointing, and no motion is possible in the orthogonal direction.

^{*} Corresponding author K. M. Lynch. Tel +1-847-467-5451. Fax +1-847-491-3915.

Email address: kmlynch@northwestern.edu (Kevin M. Lynch).

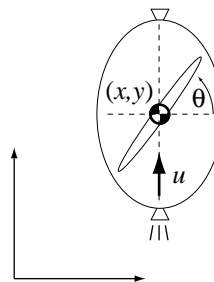


Fig. 1. The thrusting skate.

For point-to-point motions of the system, the motion planning problem is to find a curve in the configuration space (specifying the control for the skate) and a control $u(t)$ for the thruster. The optimal motion planning problem is to find controls which minimize some cost function. In this paper we are interested in energy efficient motions for a given time of motion t_f . As in [1,3,6], we search for motions that minimize

$$J = \int_0^{t_f} u(t)^2 dt. \quad (1)$$

This paper derives the optimal controls for motions between any two points at rest in the obstacle-free plane \mathbb{R}^2 . While partial results can be obtained analytically, numerical optimization is used to find the complete controls. The optimal motions can be considered analogous to the minimum-arclength paths for car-like vehicles [8] and car-like vehicles that can only go forward [2]. A car is similar to the system we study in that it has a steering control and a driving control. Unlike our system, how-

ever, the car is underactuated (nonholonomic) as the body of the car has three configuration variables (position and orientation). Another related system (though also underactuated) is the simplified snakeboard studied by Ostrowski and colleagues, which is a ground vehicle that uses steered wheels to direct the motion of the system and a momentum wheel to generate motion. Energy-optimal “gaits” for this system are derived in [7].

2 Dynamics of the Thrusted Skate

Without loss of generality, motion between any two points can be considered to be a motion between the origin and (x_f, y_f) . To nondimensionalize the analysis, the unit distance is $\sqrt{x_f^2 + y_f^2}$, unit mass is the mass of the thrusted skate, and unit time is t_f , the total time of motion.

Let v be the signed speed of the system, so the velocity can be written

$$\dot{x} = v \cos \theta \quad (2)$$

$$\dot{y} = v \sin \theta. \quad (3)$$

The controls are the steering angle $\theta \in [0, \pi)$ and the thrust u , giving the dynamics

$$\dot{v} = u \sin \theta. \quad (4)$$

Note the singularity at $\sin \theta = 0$ where the thrust u has no effect.

3 Analytical Results

Let $\mathbf{x} = (x, y, v)^T$ be the system state vector and $\mathbf{u} = (\theta, u)^T$ be the control vector. We define the system Hamiltonian

$$H = L(\mathbf{x}(t), \mathbf{u}(t), t) + \lambda(t)^T \mathbf{f}(\mathbf{x}(t), \mathbf{u}(t), t), \quad (5)$$

where L is the integrand of the objective function, $\lambda(t)$ is a Lagrange multiplier vector, and $\dot{\mathbf{x}} = \mathbf{f}(\mathbf{x}(t), \mathbf{u}(t), t)$ are the state equations. In our system, the Hamiltonian is

$$H = u^2 + \lambda_1 v \cos \theta + \lambda_2 v \sin \theta + \lambda_3 u \sin \theta. \quad (6)$$

Optimal controls satisfy the necessary condition

$$\frac{\partial H}{\partial \mathbf{u}} = 0, \quad (7)$$

and the Lagrange multipliers satisfy the co-state equation

$$\dot{\lambda} = -\frac{\partial H}{\partial \mathbf{x}}. \quad (8)$$

An optimal solution is written $\mathbf{u}^*(t), \mathbf{x}^*(t), \lambda^*(t)$.

Singular extremals may occur when Equations (7) and (8), along with the terminal conditions, provide insufficient information relating \mathbf{u}^* , \mathbf{x}^* , and λ^* . Such a situation occurs when $(x_f, y_f) = (0, 0)$; the skate may turn in place with zero cost. Goal points away from the origin do not lead to singular extremals, although, as we will see in Section 4, there may be more than one *locally* minimizing control-trajectory pair for a given goal state.

Although we cannot solve Equations (7) and (8) analytically for the extremals, we can get partial results. For our system, we have

$$\frac{\partial H}{\partial u} = 2u + \lambda_3 \sin \theta = 0 \quad (9)$$

$$\frac{\partial H}{\partial \theta} = -\lambda_1 v \sin \theta + \lambda_2 v \cos \theta + \lambda_3 u \cos \theta = 0. \quad (10)$$

From (9) we have

$$\lambda_3 = -2u / \sin \theta. \quad (11)$$

Since the motion begins and ends at rest ($v = 0$), Equation (10) implies that

$$\lambda_3 u \cos \theta = 0 \quad (12)$$

at times $t = 0$ and $t = 1$. Combining (11) and (12), we find that $-2u^2 \cot \theta = 0$ at $t = 0$ and $t = 1$. Therefore, at the beginning and end of the motion, $u = 0$ or $\cot \theta = 0$ (or both). We must have $u \neq 0$ at $t = 0$; otherwise, the state of the thrusted skate would not change, the condition would continue to hold, and the skate would remain stationary for all time. By the same reasoning, $u \neq 0$ at $t = 1$.¹ Therefore, $\cot \theta = 0$ at the beginning and end of motion — the skate is aligned with the thruster. When the skate is aligned with the thruster, the capability of the thruster to add or subtract from the system kinetic energy is maximized.

In the special case of a goal configuration at $(0, 1)$, it is possible to solve for the complete motion of the system analytically. Clearly the skate remains aligned with the thruster (and the y -axis) throughout the motion.² In this case, the Hamiltonian simplifies to

$$H' = u^2 + \lambda_2 v + \lambda_3 u \quad (13)$$

¹ Any trajectory is reversible. If $\mathbf{u}^*(t), t \in [0, 1]$ defines an optimal trajectory from $(0, 0)$ to (x_f, y_f) , then $\mathbf{u}^*(1-t), t \in [0, 1]$ defines an optimal trajectory from (x_f, y_f) to $(0, 0)$.

² One way to see this is to rewrite the cost function as $\int_0^1 (\dot{v} / \sin \theta)^2 dt$ and observe that (1) at any state \mathbf{x} , for any $\dot{v} \neq 0$, the differential cost is minimized by choosing $\sin \theta = \pm 1$; and (2) motion in the x -direction, which would require $\sin \theta \neq \pm 1$ at some point, is unnecessary for the task.

and the conditions (7) and (8) yield

$$\lambda_3 = -2u \quad (14)$$

$$\dot{\lambda}_3 = \text{constant}. \quad (15)$$

Therefore $u^*(t)$ is a linear function. $u^*(t)$ must also satisfy the terminal conditions

$$\int_0^1 u^*(t) dt = 0 \quad (16)$$

$$\int_0^1 dt \int_0^t u^*(\tau) d\tau = 1. \quad (17)$$

Solving, we get $u^*(t) = 6(1 - 2t)$. The motion of the skate is given by $y^*(t) = -2t^3 + 3t^2$, $t \in [0, 1]$, and the cost of the motion is 12. This trajectory can be verified as optimal by observing that the Hessian of the original Hamiltonian

$$H_{\mathbf{uu}} = \frac{\partial^2 H}{\partial \mathbf{u}^2} = \begin{pmatrix} 2 & \lambda_3 \cos \theta \\ \lambda_3 \cos \theta & -\lambda_1 v \cos \theta - \lambda_2 v \sin \theta - \lambda_3 u \sin \theta \end{pmatrix} \quad (18)$$

is positive definite along the trajectory. Plugging in our solution, we find

$$\text{trace}(H_{\mathbf{uu}}) = 144t^2 - 144t + 74 > 0 \quad \forall t \in [0, 1] \quad (19)$$

$$\det(H_{\mathbf{uu}}) = 144(2t^2 - 2t + 1) > 0 \quad \forall t \in [0, 1], \quad (20)$$

confirming that $H_{\mathbf{uu}}$ is positive definite along the trajectory.

4 Numerical Results

To obtain the complete optimal trajectory between two points in the plane, we resort to a numerical method. We represent the controls $u(t)$ and $\theta(t)$ by n control points spaced by $1/n$ in time. We use the sequential quadratic programming package CFSQP [4] to find the design variable vector X^* minimizing the objective function while satisfying the terminal conditions $x(1) = x_f$, $y(1) = y_f$, $\dot{x}(1) = 0$, and $\dot{y}(1) = 0$. For a given X , the objective function and the final state of the skate are calculated by exact numerical integration. Beginning from an initial guess X_0 , the gradient and an approximated Hessian of the objective and constraint functions with respect to the design variables are used to iteratively update X until convergence to a local minimum in the design variable space.

The results of the optimizations for $n = 40$ are shown in Figures 2 – 4. We chose goal points on the unit circle

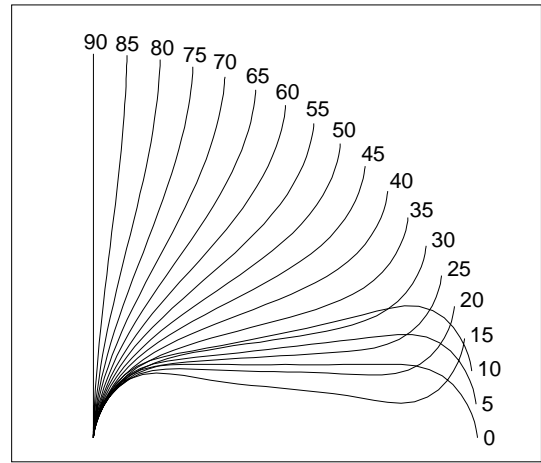


Fig. 2. The paths followed during the optimal motions. Note the two distinct types of paths, the S-curve and the U-curve.

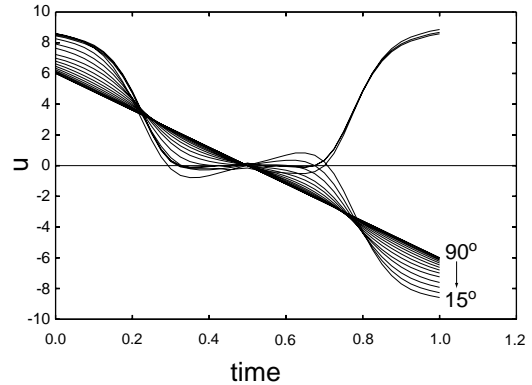


Fig. 3. The optimal thrusts for the different goal points.

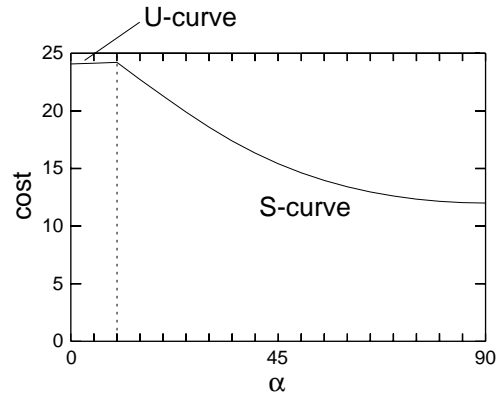


Fig. 4. The cost of the optimal motion as a function of the angle α to the terminal point. The cusp in the curve occurs at the point where the optimal path switches between the U-curve and the S-curve.

at angles α between 0° and 90° in 5° increments. The optimal controls to other points in the plane are obtained by reflecting and scaling.

Figure 2 shows the paths of the optimal motions (and,

implicitly, the steering control $\theta(t)$). Note that there are two distinct types of paths, the S-curve and the U-curve. These two types of curves correspond to two different local minima in the design space. When the angle to the goal point is small ($\alpha < 10^\circ$), the global optimum is the U-curve. For all other points, the global optimum is the S-curve. All paths start and end with motion parallel to the y -axis, as predicted by the analytical results.

Figure 3 gives the time-history of the thrust for each of the motions. For efficiency, the thrust is large when the skate is nearly aligned with the y -axis, as the thrust maximally impacts the system kinetic energy when the skate is aligned with the y -axis. When the skate is nearly aligned with the x -axis, the optimal solutions turn down the thruster and “coast” to conserve energy. When the terminal point is on the y -axis, the optimal thrust is a ramp, as predicted by the analytical results.

Figure 4 shows the cost of the optimal motion as a function of the angle α to the terminal point. The switch between global optimality of the U-curve and the S-curve is clear by the cusp in the objective function values. The most expensive motions (for small α) cost about twice as much as motion with $\alpha = 90^\circ$.

A simple approximation to the U-curve solutions is a “bang-coast-bang” strategy. For a terminal point at $(\cos \alpha, \sin \alpha)$, the skate initially moves in the $+y$ direction with constant thrust $u = u_0$ for time t_s , then coasts a distance 1 in time $1 - 2t_s$ at an angle α , then moves in the $-y$ direction with constant thrust for time t_s to decelerate to rest at the goal. A simple calculation shows that $t_s = 1/6$ and $u_0 = 9$ are the optimal choices, indicating that the pathlength of the first and third segments is 0.125. The cost of the motion is 27, within 12% of the cost for the optimal U-curves for $\alpha < 10^\circ$.

This approximation to the U-curve optimal controls can be used to find an analytical approximate solution to the cusp point of Figure 4, where the optimal solution switches from the U-curve to the S-curve. As shown in Figure 5, an approximation to the S-curve (for small α) is similar to the U-curve, with the exception that the final segment covers a distance 0.125 in the $+y$ (not $-y$) direction. The length of the intermediate segment is therefore

$$d_S = \sqrt{\cos^2 \alpha + (\sin \alpha - 0.25)^2}.$$

When $d_S < 1$, the coasting distance for the approximate S-curve is shorter than for the approximate U-curve. This indicates that less velocity is required at the end of the first segment in order to complete the coast segment in time $1 - 2t_s = 2/3$, and therefore the necessary “bang” force is less. As a result, the cost of the total motion is less. Solving, we find the approximate S-curve becomes preferable for $\alpha > 7.18^\circ$. For the full numerical results, the switch occurs closer to 10° .

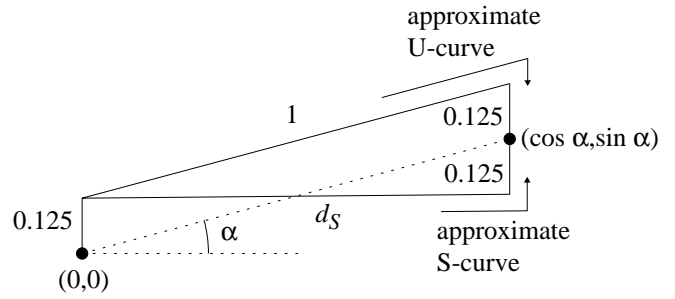


Fig. 5. The approximate U-curve path to a point $(\cos \alpha, \sin \alpha)$ consists of a length 0.125 segment along $+y$, a length 1 segment at angle α , and a length 0.125 segment along $-y$. The final segment of the S-curve approximation is length 0.125 along $+y$, and the S-curve becomes more efficient when the length d_S of the intermediate S-curve segment is less than the length one intermediate U-curve segment. This occurs for $\alpha > 7.18^\circ$.

Acknowledgments

The support of NSF grants IIS-9875469 and IIS-9811571 is gratefully acknowledged.

References

- [1] R. W. Brockett and L. Dai. Nonholonomic kinematics and the role of elliptic functions in constructive controllability. In Z. Li and J. Canny, editors, *Nonholonomic Motion Planning*. Kluwer Academic, 1993.
- [2] L. E. Dubins. On curves of minimal length with a constraint on average curvature and with prescribed initial and terminal positions and tangents. *American Journal of Mathematics*, 79:497–516, 1957.
- [3] C. Fernandes, L. Gurvits, and Z. Li. Near-optimal nonholonomic motion planning for a system of coupled rigid bodies. *IEEE Transactions on Automatic Control*, 30(3):450–463, Mar. 1994.
- [4] C. Lawrence, J. L. Zhou, and A. L. Tits. User’s guide for CFSQP version 2.3. Institute for Systems Research 94-16, University of Maryland, 1994.
- [5] C. A. Moore, M. A. Peshkin, and J. E. Colgate. Design of a 3R cobot using continuously variable transmissions. In *IEEE International Conference on Robotics and Automation*, pages 3249–3254, 1999.
- [6] R. M. Murray, Z. Li, and S. S. Sastry. *A Mathematical Introduction to Robotic Manipulation*. CRC Press, 1994.
- [7] J. P. Ostrowski, J. P. Desai, and V. Kumar. Optimal gait selection for nonholonomic locomotion systems. *International Journal of Robotics Research*, 19(3):225–237, Mar. 2000.
- [8] J. A. Reeds and L. A. Shepp. Optimal paths for a car that goes both forwards and backwards. *Pacific Journal of Mathematics*, 145(2):367–393, 1990.